iScience

CellPress
OPEN ACCESS

Article

Canagliflozin combined with aerobic exercise protects against chronic heart failure in rats

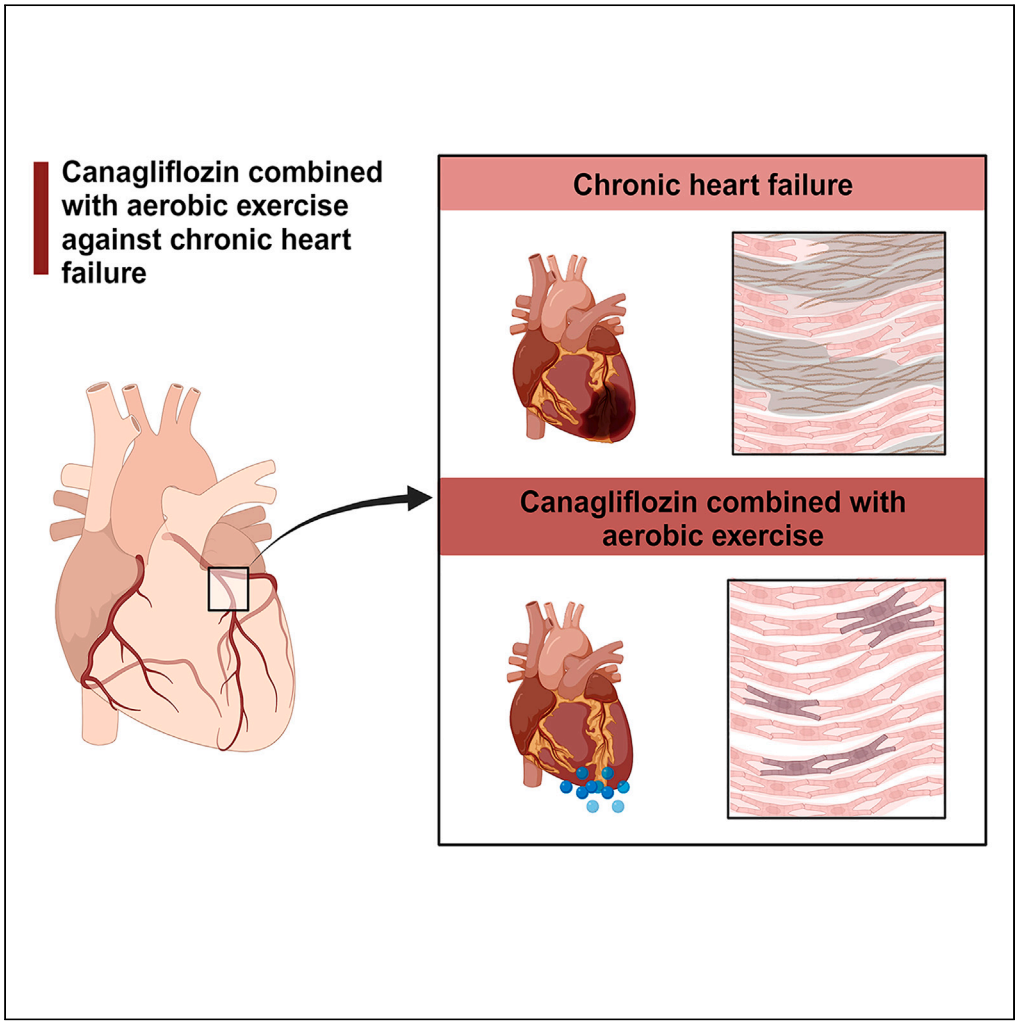

Helin Sun, Bingyu Du, Hui Fu, Zhaodi Yue, Xueyin Wang, Shaohong Yu, Zhongwen Zhang

sutcm2006@163.com (S.Y.)
zhangzhongwen@sdu.edu.cn (Z.Z.)

Highlights

Canagliflozin combined with aerobic exercise improve chronic heart failure

Canagliflozin combined with aerobic exercise reduces myocardial fibrosis

Canagliflozin combined with aerobic exercise inhibits the AKT/ERK signaling pathway

The retinol metabolism signaling pathway plays a role in chronic heart failure

Sun et al., iScience 27, 109014
March 15, 2024
https://doi.org/10.1016/j.isci.2024.109014

iScience

CellPress
OPEN ACCESS

Article

Canagliflozin combined with aerobic exercise protects against chronic heart failure in rats

Helin Sun,[1,2,6] Bingyu Du,[1,2,6] Hui Fu,[5] Zhaodi Yue,[3,4] Xueyin Wang,[2] Shaohong Yu,[3,4,*] and Zhongwen Zhang[1,2,7,*]

SUMMARY

To determine the efficacy and potential protective mechanism of canagliflozin combined with aerobic exercise in treating chronic heart failure (CHF). Isoproterenol was injected into rats to create CHF models. The rats were then subsequently divided into saline, canagliflozin (3 mg/kg/d), aerobic exercise training, and canagliflozin combined with aerobic exercise training. Compared to the CHF group, the canagliflozin combined with the aerobic exercise group had superior ventricular remodeling and cardiac function. In rats treated with canagliflozin combined with aerobic exercise, the expression of cytochrome P450 (CYP) 4A3, CYP4A8, COL1A1, COL3A1, and FN1 was reduced, while the expression of CYP26B1, ALDH1A2, and CYP1A1 increased significantly. Additionally, canagliflozin combined with aerobic exercise decreased the phosphorylation of AKT and ERK1/2. Canagliflozin combined with aerobic exercise has a positive effect on the development of CHF via the regulation of retinol metabolism and the AKT/ERK signaling pathway.

INTRODUCTION

Chronic heart failure (CHF), the most prevalent form of cardiovascular illness, is a global health issue with a high death and morbidity rate.[1] The disease affects about 2% of the adult population worldwide, and the 5-year mortality rate is estimated to be between 45 and 60%.[2] CHF is a complex condition characterized by a cardiac muscle's inability to maintain blood supply to peripheral tissues, resulting in decreased systemic energy metabolism.[3] Multiple studies have demonstrated that regulating cardiac energy metabolism is critical for treatment.[4,5] The β-oxidation of fatty acids in the mitochondria satisfies the heart's high energy requirements. Oliveros et al. observed previously observed that a vitamin A deficit paired antioxidant defenses, promoted lipid peroxidation in the adult rat heart, and altered aortic lipid metabolism.[6] The peroxisome proliferator-activated receptor (PPAR) is a ligand-activated nuclear transcription factor.[7] PPAR modulates fatty acid oxidation (FAO) and mitochondrial bioenergetics, suppresses myocardial remodeling and fibrosis, and improves HF.[8] Consequently, we must investigate new techniques for enhancing cardiac function by ameliorating abnormalities of cardiac energy metabolism, preventing cardiac remodeling and fibrosis, and thereby preventing or postponing the advancement of heart failure.

Canagliflozin, an inhibitor of sodium-glucose cotransporter 2 (SGLT-2), has been demonstrated to benefit HF with a lower ejection fraction.[9] SGLT-2 inhibitors (canagliflozin, and so forth) for patients with CHF, improve the quality of life, and reduce mortality, morbidity, and readmission rates.[10] In diabetic and nondiabetic subjects, canagliflozin treatment significantly reduced the risk of cardiovascular death, myocardial infarction, and hospitalization for hypertension.[11] In addition, SGLT-2 inhibitors can improve fatty acid metabolism and utilize ketone bodies to create mitochondrial energy, so enhancing the aerobic metabolism of skeletal muscle, inhibiting anaerobic metabolism, and enhancing aerobic exercise capacity.[12] Canagliflozin has been demonstrated to decrease myocardial glucose metabolism, enhance myocardial fatty acid metabolism, and increase the circulation of ketone bodies,[13] thereby ameliorating heart failure via modifying myocardial energy metabolism and oxidative stress.[14]

Aerobic exercise training is associated with improved aerobic capacity, cardiovascular function, and metabolic regulation.[15] In patients with CHF, aerobic exercise positively benefits cardiovascular function, myocardial metabolism, and antioxidant status.[16] Additionally, it can effectively reverse ventricular remodeling in heart failure, enhance aerobic capacity, and maximal oxygen absorption.[17] The proposed mechanisms of aerobic exercise in the therapy of CHF include increased energy expenditure and improved metabolic function. Tomas et al. demonstrated that moderate-intensity aerobic exercise boosted mitochondrial respiration, ATP levels, and cardiac function in rats

[1]Department of Endocrinology and Metabology, Shenzhen Research Institute of Shandong University, Shenzhen, China, Shandong Provincial Key Laboratory for Rheumatic Disease and Translational Medicine, The First Affiliated Hospital of Shandong First Medical University & Shandong Provincial Qianfoshan Hospital, Jinan, China
[2]Department of Endocrinology and Metabology, The Third Affiliated Hospital of Shandong First Medical University & Shandong Academy of Medical Sciences, Jinan, China
[3]Teaching and Research Section of Internal Medicine, College of Medicine, Shandong University of Traditional Chinese Medicine, Jinan, China
[4]Department of rehabilitation medicine, The Second Affiliated Hospital of Shandong University of Traditional Chinese Medicine, Jinan, China
[5]Cheeloo College of Medicine, Shandong University, Jinan, China
[6]These authors contributed equally
[7]Lead contact
*Correspondence: sutcm2006@163.com (S.Y.), zhangzhongwen@sdu.edu.cn (Z.Z.)
https://doi.org/10.1016/j.isci.2024.109014

with CHF.[18] Also, aerobic exercise has been shown to stimulate the release of irisin in cardiomyocytes, thereby enhancing cardiomyocyte metabolism, preserving mitochondrial function, and increasing energy expenditure.[19]

The 2021 Canadian Heart Failure Guidelines highlight the combination of prescribed medications (SGLT-2 inhibitors, beta-blockers, and so forth) and nonpharmacological therapy for the treatment of CHF.[10,20] Based on canagliflozin medication, combined aerobic exercise may be more beneficial in treating CHF, but the particular effect and molecular mechanism remain unknown. This study was designed to examine the efficacy and potential protective mode of action of canagliflozin combined with aerobic exercise in the treatment of CHF.

MATERIALS AND METHODS

Experimental animals

Male Sprague Dawley (SD) rats of eight weeks of age were acquired from Beijing Weitong Lihua Laboratory Animal Technology Co., Ltd., and animal experiments were conducted in the SPF animal room of the First Affiliated Hospital of Shandong First Medical University (License number: SCXK Beijing 2016-0006). Before the experiment, the rats were housed for two weeks under standard temperature (21–23°C) and humidity (40–60%) conditions with free access to food and drink. The care and use of laboratory animals conformed to the Guide for the Management and Use of Laboratory Animals, and the Animal Experimentation Committee of the First Affiliated Hospital of Shandong First Medical University granted ethical and scientific approval (2020S014).

Experimental protocol

70 rats were randomly assigned to two groups: the saline-treated control group (n = 6) and the CHF group (n = 64). As previously stated,[21] the isoproterenol (ISO)-induced rat models of CHF were created. For ten days, rats were injected intra-peritoneally with a 5 mg/kg/d ISO solution. Animals that have died were excluded from the study. After establishing the model, 24 rats in the CHF group survived and were randomized into four groups: the ISO+CA group (n = 6, oral administration of canagliflozin 3 mg/kg/d), the ISO+AE group (n = 6, aerobic exercise training on a small animal multitrack treadmill), the ISO+AE+CA group (n = 6, simultaneous oral administration of canagliflozin and aerobic exercise training), and the ISO group (n = 6, oral administration of equal amounts of normal saline).

Regarding the study by HIRA et al.,[22] canagliflozin (Merck Serono, Beijing, China) was supplied through gavage, and the medication dose was established to be 3 mg/kg/d for 4 weeks. The aerobic exercise program is based on the design of Bedford et al.[23] Every day, rats completed 5 to 10 min of warm-up exercise (speed 5 m/min, incline 0°), after which the speed was increased to 12 m/min and the elevation was altered to 5° (equivalent to 45 percent VO2max). On days 1, 2, and 3, the running time was 15, 30, and 45 min, respectively, and on day 4, the running time was increased to 60 min. The aerobic exercise was performed six times each week for four weeks. The study excluded rats who refused to run steadily on the treadmill. After four weeks, the rats were anesthetized with 2% sodium pentobarbital (40 mg/kg) and sacrificed. Blood was obtained from the femoral artery, centrifuged to collect serum, and then stored at −80°C for ELISA. Cardiac tissue samples taken from the mid LV (2.5 mm above the apex) of the heart were fixed with 4% paraformaldehyde for histopathological analysis and immunohistochemical staining, and the remaining LV tissues were stored at −80°C for western blot assay and qPCR analysis.

Echocardiographic assessment

Echocardiography was performed one day before the ISO injection, one day after the ISO injection, and four weeks after the drug and exercise interventions. To alleviate pain and anxiety, rats were sedated with 1.5% isoflurane and placed in the supine position. Left ventricular ejection fraction (LVEF) and left ventricular fractional shortening (LVFS) were the key parameters measured. Parameters such as the left ventricular end of systole volume (LVESV), left ventricular end of diastole volume (LVEDV), left ventricular internal diameter at end-systole (LVID), left ventricular internal diameter at end-diastole (LVIDd), left ventricular posterior wall diastole (LVPWd), left ventricular posterior wall systole (LVPWs), left ventricular anterior wall diastole (LVAWd), and left ventricular anterior wall systole (LVAWs) were obtained from the 2D-guided M-mode measurements by software of the Vevo 3100 (VisualSonics Inc, Toronto, Ontario, Canada). The values of LVFS and LVEF were calculated by the Vevo LAB software. Carry out three measurement analyses and take the average value of the three analyses.

Histopathological examination

After immobilizing myocardial tissues with 4% paraformaldehyde for at least 48 h, paraffin sections were prepared. These sections were stained with hematoxylin-eosin (HE) and Masson trichrome to evaluate histopathological alterations and collagen deposition, then photographed at a magnification of 40×. Using Image-Pro Plus 6.0, the collagen volume fraction (collagen area/total area × 100%) was calculated.

Immunohistochemistry

The hearts were submerged in paraformaldehyde at a concentration of 4% and embedded in paraffin. Cross-sections of the heart were dewaxed, heated for antigen retrieval, treated with 3 percent hydrogen peroxide to inhibit endogenous peroxidase activity, and then blocked with 4 percent bovine serum albumin. The sections were then treated overnight at 4°C with the primary antibodies collagen I (COL1) (Abcam, 1:150), collagen III (COL3) (Abcam, 1:700) and fibronectin (FN1) (Abcam, 1:1000). The slices were treated with the appropriate secondary antibodies, and the positive staining was detected with diaminobenzidine (DAB) and counterstained with hematoxylin before being studied under a 40-magnification electron microscope. Image Pro Plus 6.0 software was used to quantify every image.

RNA sequencing

Total RNA was extracted from the apical tissue using the RNeasy Mini Kit (250) Qi-agen#74106 kit, and three biological replicates in the Control, ISO, ISO+CA, and ISO+AE+CA groups were used for quality inspection and RNA quantification. Strand-specific libraries were prepared following the depletion of ribosomal RNA and sequenced on an Illumina NovaSeq 6000 instrument using the paired-end sequencing chemistry.

The raw off-machine data were first processed to obtain high-quality sequences, and then the high-quality sequences were aligned to reference genes, and the results were quantified for transcriptome expression. Differentially expressed genes were calculated and differentially screened by Fragments Per Kilobase per Million (FPKM), and so forth. Screening criteria: p value < 0.05 and the fold change (FC) is 2 times up (FC $\geq$ 2) or 2 times down (FC $\leq$ 2) 0.5) and eliminated the differentially expressed genes with FPKM less than 1 in each group. Visual analysis of sequencing results using R language and bioinformatics online tools (http://www.bioinformatics.com.cn/). The STRING 11.5 database[24] (https://cn.string-db.org) contains genes with distinct expressions. After hiding unconnected nodes, platform and protein-protein interaction (PPI) networks were obtained. To further examine the PPI network, the Molecular Complex Detection (MCODE) [25] tool of Cytoscape 3.7.1[26] (http://cytoscape.org/) was utilized. Gene Ontology (GO) functional analysis and Kyoto Encyclopedia of Genes and Genomes (KEGG) enrichment analysis were performed using Metascape[27] (https://metascape.org/), and bioinformatics online tools and Cytoscape 3.7.1 software were utilized for data visualization.

Western blot analysis

Protein lysates from heart tissue were separated by 10% SDS-PAGE and then transferred to PVDF membranes (EMD Millipore, Billerica, MA, USA). Membranes were incubated overnight at 4°C with the following primary antibodies: β-tubulin (1:1,000; 10068-1-AP; Proteintech), AKT (1:1,000; cat. no. ab32505; Abcam), phosphorylated AKT (*p*-AKT) (1:1,000; cat. no. ab192623; Abcam), ERK1/2 (1:1,000; cat. no. ab184699; Abcam), and phosphorylated ERK1/2 (1:1,000; cat. no. ab201015; Abcam). The membranes were cleaned and incubated with the appropriate secondary antibody (1:10000) at room temperature for 1 h the following day. Using an ECL Chemiluminescence Kit, blots were seen (servicebio, Wuhan, China). Using the FluorChem E imaging equipment, the protein bands were semi quantified (ProteinSimple, San Francisco, CA, USA). Using an image analysis system, protein band densities were assessed and expressed as ratios to AKT or ERK1/2.

Quantitative reverse transcription-PCR analysis

Total RNA was extracted using TRIzol reagent (Genstar, Beijing, China) according to the manufacturer's protocol, and cDNA was obtained by reverse transcription reaction with *mRNA* utilizing an AccuPower RT PreMix kit (Accurate Biology, Hunan, China). Quantitative real-time PCR (qPCR) was used to determine the *mRNA* levels of collagen 1 alpha 1 (COL1A1), collagen 3 alpha 1 (COL3A1), FN1, cytochrome P450 (CYP) 1A1, CYP2C23, CYP4A8, CYP4A3, CYP26B1, Aldehyde oxidase 1 (AOX1), Aldehyde dehydrogenase 1 family member A2 (ALDH1A2). As an internal control, β-actin was used to calculate relative expression. The relative RNA concentration was determined using the $2^{-\Delta\Delta ct}$ method.

Enzyme-linked immunosorbent assay analysis

After four weeks of intervention, blood samples from rats were collected. ELISA kits were used to determine the serum concentrations of N-terminal pro-B-type natriuretic peptide (NT-pro BNP) (Shanghai Enzyme-linked Biotechnology Co., Ltd.) according to the manufacturer's instructions.

Statistical analysis

GraphPad Prism 8 software (GraphPad, SanDiego, CA, USA) was used to analyze the data, and the results are presented as mean $\pm$ standard errors of mean (SEM). For multivariate comparisons between groups, a two-way ANOVA followed by the Turkey post–hoc test was used. $p < 0.05$, $p < 0.01$, $p < 0.001$, and $p < 0.0001$ were considered to be statistically significant.

RESULTS

Canagliflozin combined with aerobic exercise improved isoproterenol-induced cardiac dysfunction

To investigate the effect of canagliflozin combined with aerobic exercise on CHF, cardiac function was assessed using echocardiography. After 10 days of ISO administration, the levels of LVEF ($p < 0.001$) and LVFS ($p < 0.001$) in the ISO group were significantly lower than in the control group, indicating that the CHF rat model was successfully established. LVEF and LVFS levels were significantly higher in the ISO+CA group (LVEF, $p < 0.05$; LVFS, $p < 0.05$), the ISO+AE group (LVEF, $p < 0.05$; LVFS, $p < 0.05$), and the ISO+AE+CA group (LVEF, $p < 0.01$; LVFS, $p < 0.01$). Moreover, compared to the ISO group, the levels of LVIDs ($p < 0.05$) and LVESV ($p < 0.05$) were significantly reduced in the ISO+AE+CA group but not in the ISO+CA group (LVIDs, $p = 0.21$; LVESV, $p = 0.21$). (Figures 1A and 1B, Table 1).

To further confirm the protective effect of canagliflozin combined with aerobic exercise on CHF, NT-pro BNP serum levels were measure.[28] Compared to the ISO group, the NT-pro BNP levels in the ISO+AE group ($p < 0.01$), the ISO+CA group ($p < 0.05$), and the ISO+AE+CA group

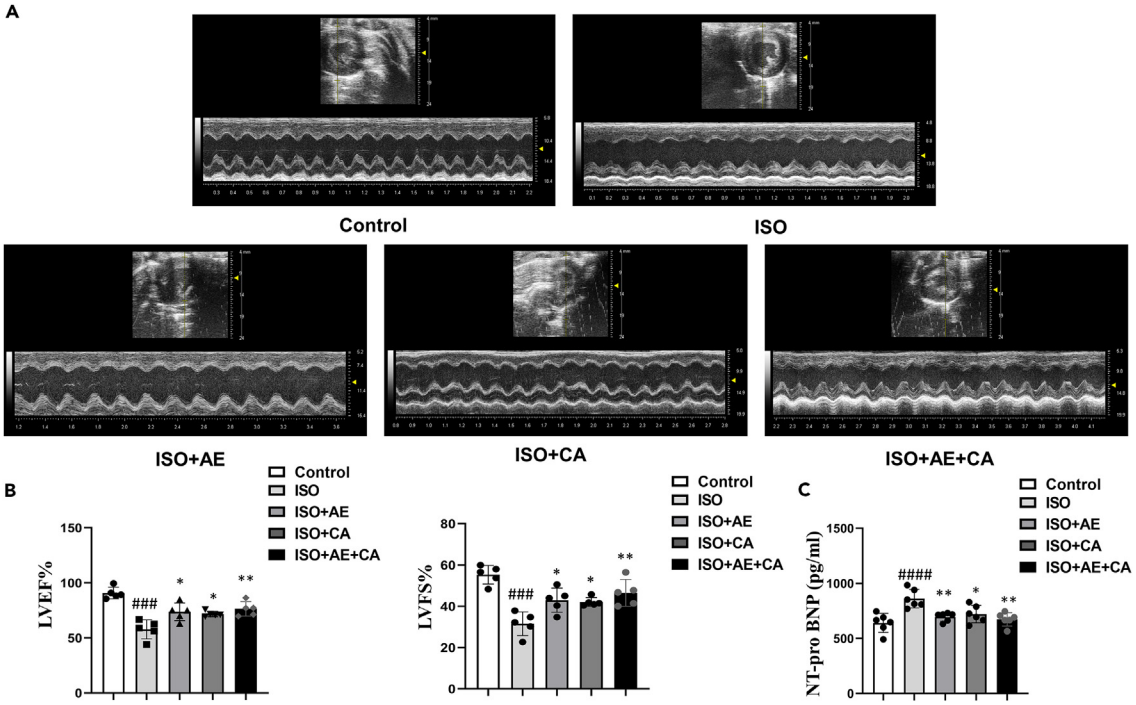

Figure 1. Effects of canagliflozin combined with aerobic exercise on echocardiographic variables in rats induced by ISO

(A) The representative images of echocardiography in different groups.

(B) The quantitative results of echocardiography.

(C) The expression level of NT-pro BNP. Data are shown as the mean ± SEM of n = 5 per group. Significance: ###p < 0.001 vs. control group; ####p < 0.0001 vs. control group; *p < 0.05 vs. ISO group; **p < 0.01 vs. ISO group. ISO, isoproterenol-treated group; ISO + AE, ISO + aerobic exercise group. ISO + CA, ISO + canagliflozin; ISO + AE + CA, ISO + aerobic exercise + canagliflozin; LVEF, left ventricular ejection fraction; LVFS, left ventricular fractional shortening; NT-pro BNP, N-terminal pro-B-type natriuretic peptide. Data are represented as mean ± SEM.

(p < 0.01) were significantly lower (Table 1). These results suggested that ISO impaired cardiac function and that canagliflozin intervention alone and in combination with aerobic exercise therapy improved ISO-induced cardiac insufficiency by enhancing myocardial contractility.

Canagliflozin combined with aerobic exercise can improve isoproterenol-induced ventricular remodeling

We used HE and Masson trichrome staining to determine the effects of canagliflozin in conjunction with aerobic exercise on ISO-induced pathological morphology and collagen fiber deposition in rat hearts.

Table 1. Canagliflozin combined with aerobic exercise improved left ventricular function in ISO-induced rats

Group	Control	ISO	ISO+AE	ISO+CA	ISO+CA+AE
LVPWd (mm)	2.64 ± 0.47	2.33 ± 0.12	2.42 ± 0.26	2.28 ± 0.16	2.46 ± 0.17
LVPWs (mm)	3.31 ± 0.35	3.35 ± 0.26	3.56 ± 0.35	3.76 ± 0.17	3.92 ± 0.23
LVAWd (mm)	2.74 ± 0.22	2.05 ± 0.21	2.23 ± 0.13	2.17 ± 0.15	2.49 ± 0.20
LVAWs (mm)	4.04 ± 0.06	2.71 ± 0.20##	3.14 ± 0.24	2.99 ± 0.10	3.21 ± 0.32
LVIDd (mm)	7.11 ± 0.31	6.73 ± 0.04	6.09 ± 0.30	7.01 ± 0.39	6.64 ± 0.61
LVIDs (mm)	2.86 ± 0.38	4.16 ± 0.28##	2.67 ± 0.25***	3.56 ± 0.26	3.39 ± 0.32*
LVEDV (ul)	272.20 ± 29.05	248.80 ± 7.02	159.40 ± 18.84***	260.10 ± 32.15	237.00 ± 54.53
LVESV (ul)	60.15 ± 11.05	111.40 ± 18.51##	43.03 ± 8.68***	74.01 ± 10.62	56.47 ± 13.57**

ISO, isoproterenol-treated group; ISO + AE, ISO + aerobic exercise group; ISO + CA, ISO + canagliflozin; ISO + AE + CA, ISO + aerobic exercise + canagliflozin; LVPWd, left ventricular posterior wall thickness at end-diastole; LVPWs, left ventricular posterior wall thickness at end systole; LVAWd, left ventricular anterior wall diastole; LVAWs, left ventricular end systolic anterior wall thickness; LVIDd, left ventricular end-diastolic inner-dimension; LVIDs, left ventricular end-systolic inner-dimension; LVEDV, left ventricular end-diastolic volume; LVESV, left ventricular end-systolic volume. The results are expressed as mean ± SEM of n = 5 per group. Significance: #p < 0.05 vs. control group; ##p < 0.01 vs. control group; ####p < 0.0001 vs. control group; *p < 0.05 vs. ISO group; **p < 0.01 vs. ISO group; ***p < 0.001 vs. ISO group. Data are represented as mean ± SEM.

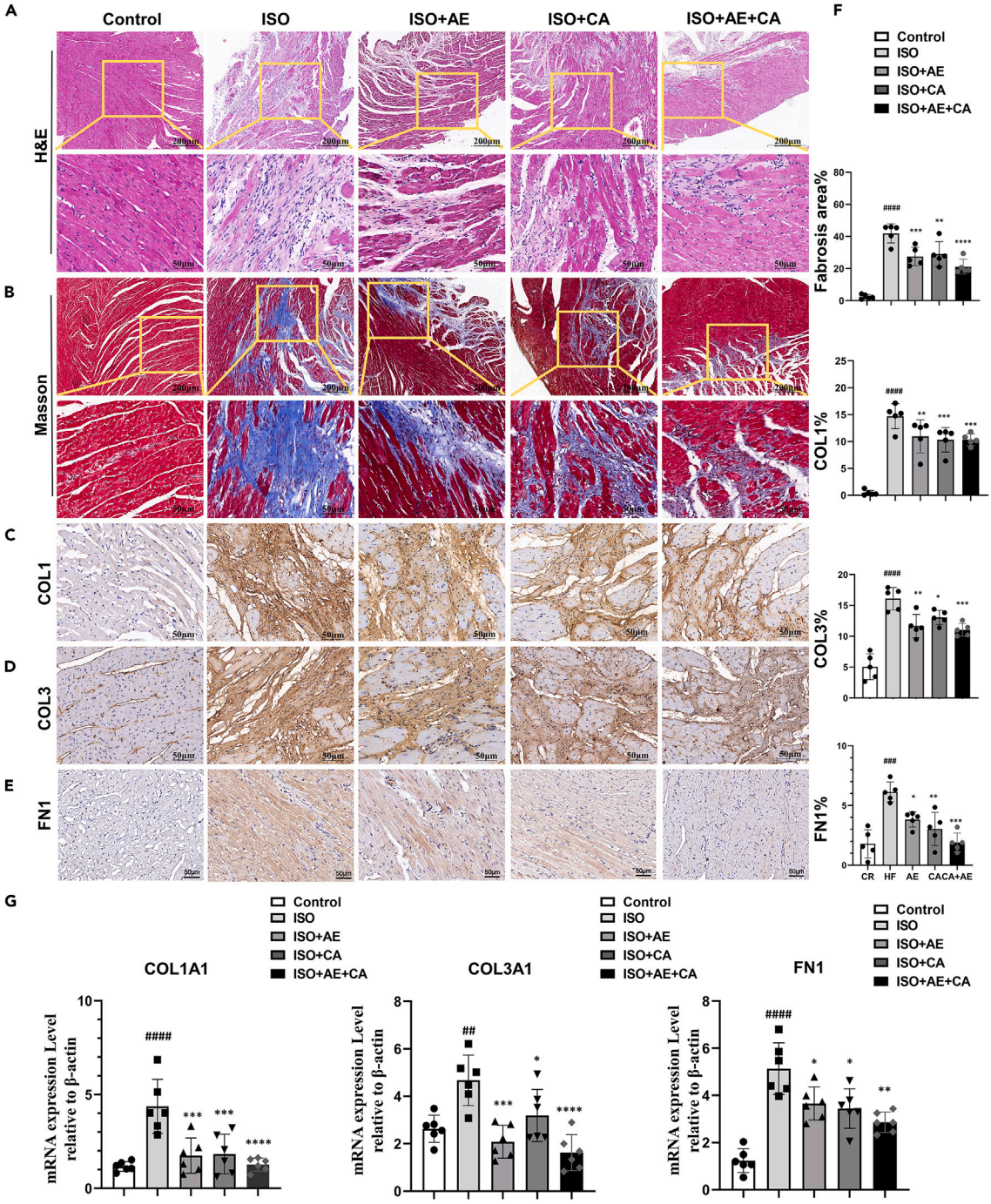

Figure 2. Effects of canagliflozin combined with aerobic exercise on ventricular remodeling in rat heart tissue

(A) Representative images of HE staining of left ventricular tissue in different groups (Microscope magnification 10×, scale bar indicates 200 μm; Microscope magnification 40×, scale bar indicates 50 μm).

(B) Representative images of Masson trichrome staining of left ventricular tissue in different groups, (Microscope magnification 10×, scale bar indicates 200 μm; Microscope magnification 40×, scale bar indicates 50 μm).

(C–E) Immunohistochemical analysis of collagen I, collagen III and fibronectin protein in heart cross sections of different groups (Microscope magnification 40×, scale bar indicates 50 μm).

(F) The quantitative analysis of collagen deposition and percentage area of collagen I, collagen III and fibronectin.

Figure 2. *Continued*

(G) The gene expression levels of COL1A1, COL3A1 and FN1 were detected by qPCR. The internal reference was β-actin. Data are shown as the mean ± SEM of n = 5–6 per group. Significance: ###p < 0.001 vs. control group; ####p < 0.0001 vs. control group; ***p < 0.001 vs. ISO group; ****p < 0.0001 vs. ISO group. ISO, isoproterenol-treated group; ISO + AE, ISO + aerobic exercise group; ISO + CA, ISO + canagliflozin; ISO + AE + CA, ISO + aerobic exercise + canagliflozin; HE, hematoxylin-eosin; COL1, Collagen I; COL3, Collagen III; FN1, fibronectin. Data are represented as mean ± SEM.

Figure 2A demonstrates that the cardiomyocytes in the ISO group were significantly sparse and hypertrophied, the myocardial fibers were broken and disorganized. With a relatively neat arrangement of myocardial fibers, the pathological histological changes of the rats in the ISO+AE+CA group were improved. As depicted in Figures 2B and 2F, Masson trichrome staining revealed that collagen fiber deposition was significantly elevated in the ISO group ($p < 0.0001$) compared to the control group. The deposition of collagen fibers was significantly reduced in the ISO+AE group ($p < 0.001$), the ISO+CA group ($p < 0.01$), and the ISO+AE+CA group ($p < 0.0001$) compared to the ISO group. Intervention with canagliflozin alone or combined with aerobic exercise therapy improved myocardial pathological changes and decreased collagen fiber deposition.

To examine the potential modulating effect of canagliflozin combined with aerobic exercise therapy on myocardial fibrosis, the immunohistochemical expression of the fibrosis markers COL1, COL3, and FN1 was measured. As shown in Figures 2C–2E, quantitative image analysis revealed a significant increase in COL1 ($p < 0.0001$), COL3 ($p < 0.0001$), and FN1 ($p < 0.05$) expression in the ISO group compared to the control group. Compared with the ISO group, the expression of COL1, COL3 and FN1 in the ISO+AE group (COL1, $p < 0.01$; COL3, $p < 0.01$; FN1, $p < 0.01$), ISO+CA group (COL1, $p < 0.001$; COL3, $p < 0.05$; FN1, $p < 0.05$) and ISO+AE+CA group (COL1, $p < 0.001$; COL3, $p < 0.001$; FN1, $p < 0.05$) were significantly reduced.

RT-PCR was used to confirm the differential expression of genes associated with fibrosis. As shown in Figure 2G, The *mRNA* levels of COL1A1 ($p < 0.0001$), COL3A1 ($p < 0.01$) and FN1 ($p < 0.001$) were significantly up-regulated in the ISO group compared with the control group, whereas the expression of COL1A1, COL3A1 and FN1 genes were down-regulated in the ISO+AE group (COL1A1, $p < 0.001$; COL3A1, $p < 0.001$; FN1 $p < 0.05$), the ISO+CA group (COL1A1, $p < 0.001$; COL3A1, $p < 0.05$, FN1< 0.05), and the ISO+AE+CA group (COL1A1, $p < 0.0001$; COL3A1, $p < 0.0001$; FN1, $p < 0.01$), compared with the ISO group. These results suggested that both canagliflozin intervention and combined aerobic exercise training can reduce myocardial fibrosis.

Canagliflozin combined with aerobic exercise attenuated isoproterenol-induced chronic heart failure in rats mainly by the retinol metabolism signaling pathway

The cardiac transcriptome of the control, ISO, ISO+CA, and ISO+AE+CA groups were profiled and qPCR was used to validate the sequencing data. We focused our analysis on the sequencing results of the ISO group versus the Control group and ISO+AE+CA group versus the ISO group. RNA-seq detected 18,713 genes in the apical tissue of the ISO groups and Control group, there were 19,091 genes in the apical tissue of the canagliflozin combined with aerobic exercise treatment and ISO groups, with 152 differentially expressed genes, including 51 up-regulated and 101 down-regulated genes (Figure 3). From the PPI network, an MCODE module consisting of 6 targets was identified, which may play more significant regulatory roles (Figure 4A).

Figure 4B depicts the biological process items from the differentially expressed genes' GO analysis. Down-regulated genes were associated with response to vitamin A, retinoic acid metabolic process, positive regulation of icosanoid secretion, and regulation of icosanoid secretion. Up-regulated genes were predominantly involved in the collagen metabolic process, response to organophosphorus, response to retinoic acid, and diterpenoid metabolic process. Most involved in the retinol metabolism, PI3K-Akt signaling pathway, AGE-RAGE signaling pathway in diabetic complications, and TNF signaling pathway, according to the KEGG pathway enrichment analysis (Figure 4C). Intriguingly, the majority of the differentially expressed genes were enriched in the retinol metabolism pathway, and the GO analysis also included responses to vitamin A and the retinoic acid metabolic process. Therefore, we hypothesized that the combination of canagliflozin and aerobic exercise could improve CHF primarily via the retinol metabolism pathway.

Based on the results of the KEGG pathway enrichment analysis, a target pathway network was constructed using Cytoscape 3.7.1 (Figure 4D). CYP4A3, CYP4A8, ALDH1A2, CYP26B1, CYP1A1, and AOX1 in the protein functional module were enriched in the retinol metabolic pathway, consequently, these six targets were deemed essential for further qPCR validation. As shown in Figures 5A and 5B, relative to the control group, the *mRNA* levels of CYP4A3 ($p < 0.05$), CYP4A8 ($p < 0.0001$), and AOX1 ($p < 0.0001$) in the ISO group were significantly up-regulated, while ALDH1A2 ($p < 0.01$), CYP26B1 ($p < 0.05$) and CYP1A1 ($p < 0.01$) were significantly down-regulated. By treating with canagliflozin alone (CYP4A3, $p < 0.05$; CYP4A8, $p < 0.0001$), aerobic exercise alone (CYP4A3, $p < 0.05$; CYP4A8, $p < 0.001$), or in combination with aerobic exercise (CYP4A3, $p < 0.0001$; CYP4A8, $p < 0.0001$), the *mRNA* levels of CYP4A3 and CYP4A8 were significantly down. In addition, canagliflozin combined with aerobic exercise significantly upregulated the levels of ALDH1A2 ($p < 0.001$), CYP1A1 ($p < 0.05$), and CYP26B1 ($p < 0.001$). As expected, the qPCR results were largely congruent with those of RNA-seq, demonstrating the precision of the high-throughput RNA-seq results.

Canagliflozin combined with aerobic exercise exerted the protective effect against CHF by inhibiting the activation of the AKT/ERK signaling pathway.

AKT/ERK signaling pathways that are activated can exacerbate myocardial fibrosis.[29–31] Our preliminary sequencing results indicated that the biological process analysis of the down-regulated genes includes components that regulate the activity of protein kinase. To determine whether the activation was inhibited by the combination of canagliflozin and aerobic exercise, the phosphorylation status of the AKT and ERK

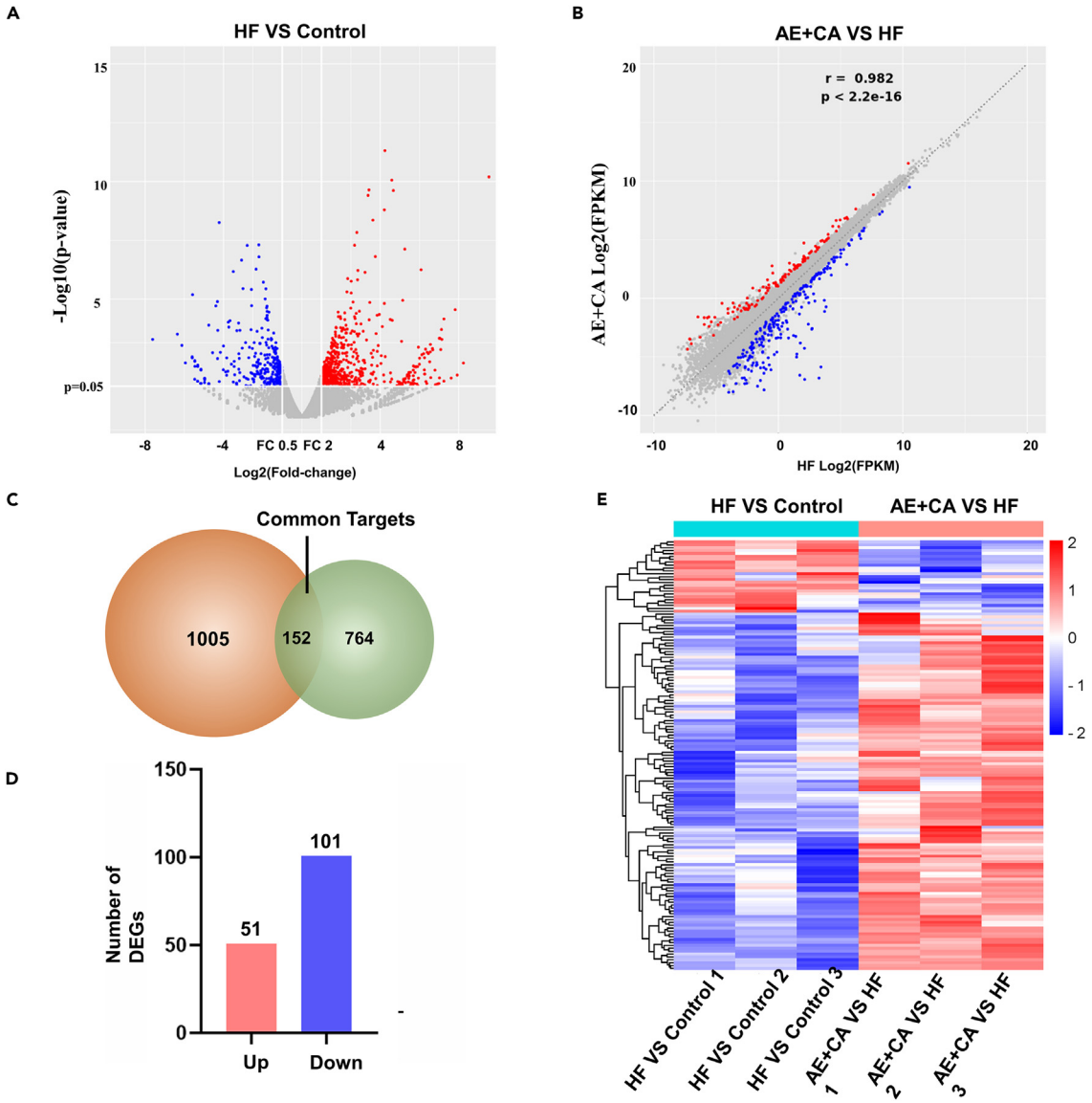

Figure 3. RNA-seq was performed to detect genome-wide transcriptomes and identify differentially expressed genes

(A) Volcano plot of differential genes from the ISO group and the Control group identified through RNA-seq. The abscissa is log2 (fold change), and the vertical coordinate is the negative logarithm of the value of Q with a base of 10, i.e., -log10 (Q). The larger the value, the more significant the difference.

(B) Scatterplot of differential genes. The horizontal and vertical coordinates represent the samples from the ISO group and the ISO+AE+CA group, respectively. The red indicates the up-regulated differential genes in the ISO+AE+CA group relative to the ISO group and the blue indicates the down-regulated differential genes in the AE + CA group relative to the ISO group, and the gray indicates genes that are not different between the two groups.

(C) Venn diagram. The orange section indicates differential genes from the ISO group and the Control group targets, and the green section indicates differential the ISO group and the ISO+AE+CA group targets. One hundred and fifty-two targets in the middle overlapping section are common targets.

(D) Histogram of differential genes.

(E) Heatmap of differential genes. Each row represents a differential gene, each column represents the same rat sample, and each group has 3 replicates.

signaling pathway was determined using Western blotting. The basal levels of AKT and ERK1/2 did not differ significantly between groups. However, compared to the control group, the *p*-AKT/AKT ratio ($p < 0.0001$) and *p*-ERK1/2/ERK1/2 ratio ($p < 0.0001$) were elevated in the ISO group indicating that ISO stimulation activated the AKT/ERK signaling pathway in rats. Compared to the ISO group, the *p*-AKT/AKT ratio and the *p*-ERK1/2/ERK1/2 ratio were significantly decreased in the ISO+CA group (*p*-AKT/AKT, $p < 0.01$; *p*-ERK1/2/ERK1/2, $p < 0.001$), ISO+AE group (*p*-AKT/AKT, $p < 0.01$; *p*-ERK1/2/ERK1/2, $p < 0.001$) and a combination of both (*p*-AKT/AKT, $p < 0.0001$; *p*-ERK1/2/ERK1/2, $p < 0.001$). These findings supported the conclusion that canagliflozin treatment alone or in conjunction with aerobic exercise may be cardioprotective by inhibiting AKT/ERK pathway activation (Figure 6).

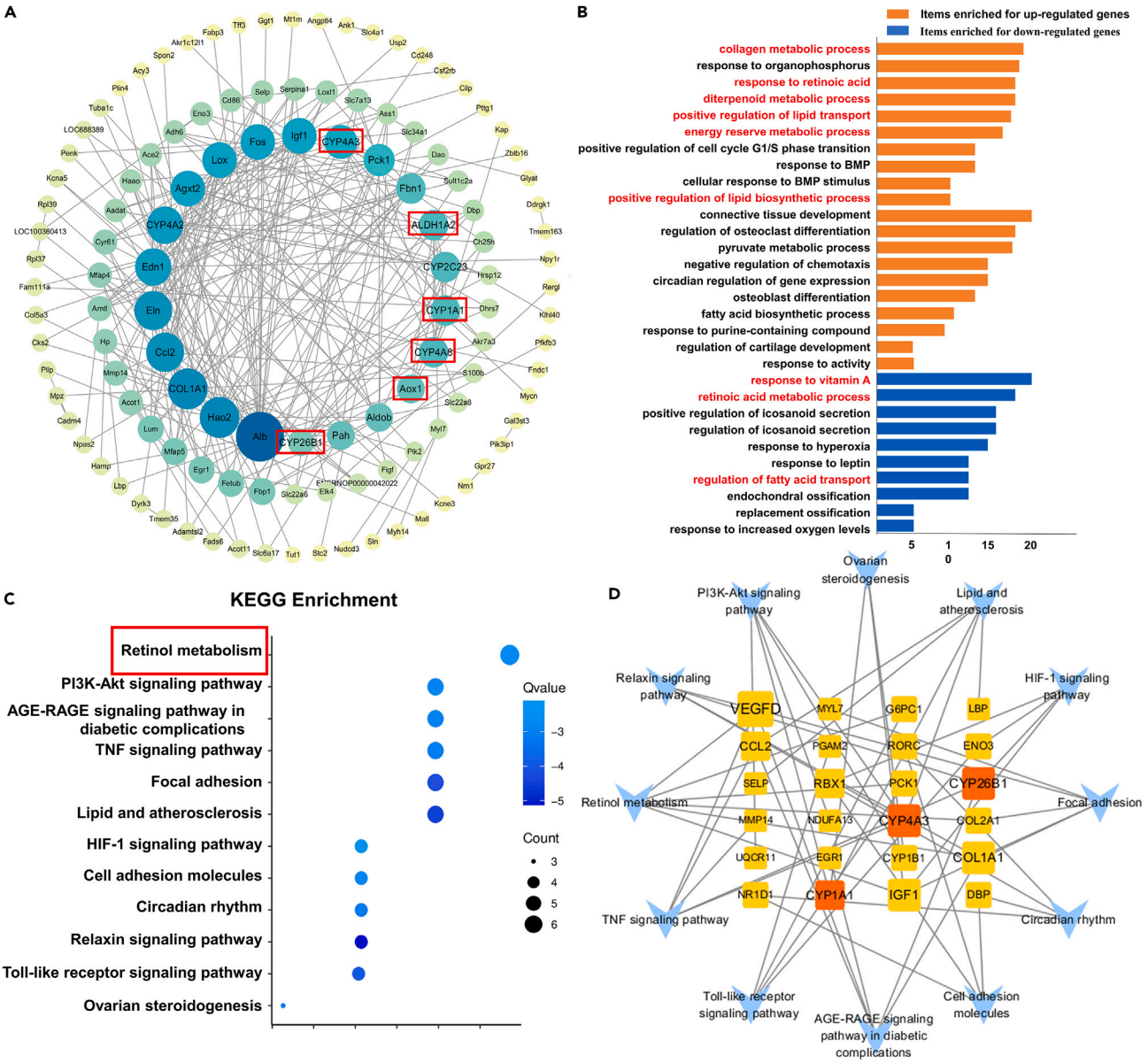

Figure 4. Enrichment analysis of the targets of canagliflozin combined with aerobic exercise in treating CHF

(A) PPI network. A total of 120 target proteins and 258 interacting edges are in the network. The sizes and colors of the nodes are illustrated from big to small and blue to green in descending order of degree values.

(B) GO functional analysis. Biological process items in GO analysis enriched for up-regulated and down-regulated genes respectively.

(C) KEGG pathway enrichment analysis. The sizes of the bubbles were illustrated from big to small in descending order of the number of potential targets involved in the pathways.

(D) Target-pathway network. A total of 36 nodes and 54 edges are in the network. The middle square nodes represent targets on the pathway, the red nodes represent key targets, and 12 blue V-shapes represent pathways. The sizes of the square node were illustrated from big to small in descending order of degree values. 54 edges represent the interaction relationship between components, targets, and pathways. CHF, chronic heart failure; PPI, protein-protein interaction; GO, Gene Ontology; KEGG, Kyoto Encyclopedia of Genes and Genomes.

DISCUSSION

CHF is a complex end-stage of multiple cardiovascular diseases caused by diastolic or systolic heart dysfunction.[32] Given that the pathogenesis of CHF is associated with a variety of factors, including neurohormonal activation, ventricular remodeling, and disturbances in energy metabolism,[2] multi-target and multi-pathway therapy may be more effective for the treatment of CHF. In the present study, we first confirmed that canagliflozin combined with aerobic exercise treatment could improve cardiac function and myocardial fibrosis. Incorporating network

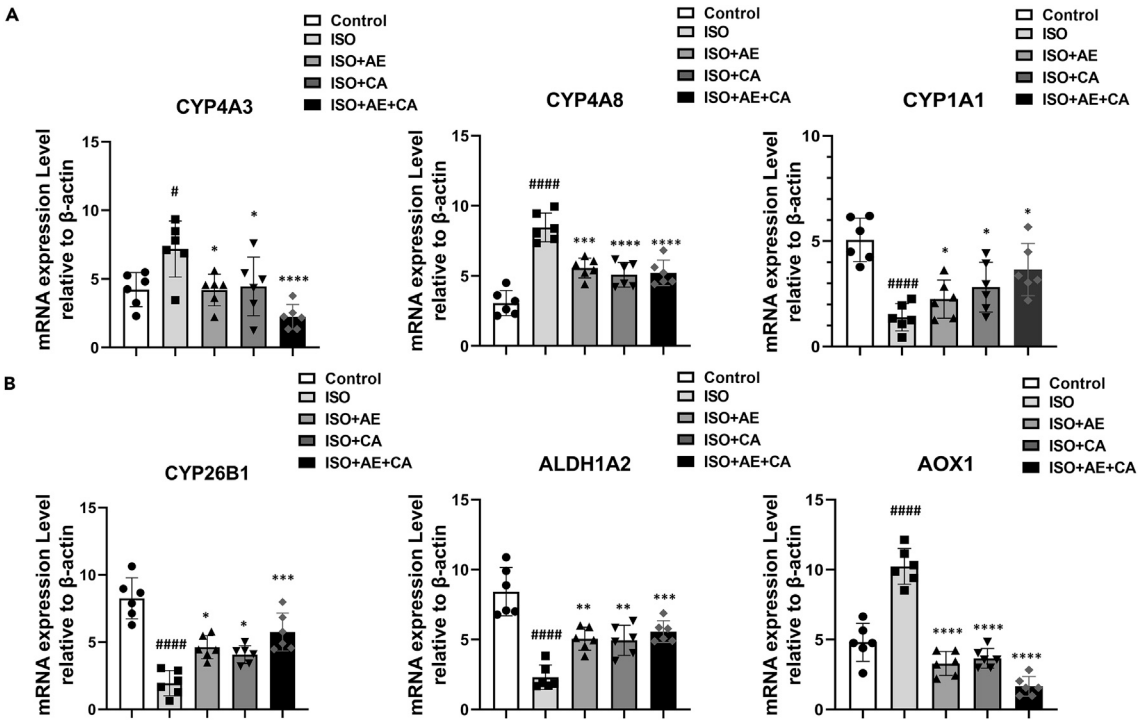

Figure 5. Effects of canagliflozin combined with aerobic exercise on retinol metabolic pathways and indicators of fibrosis

(A) The gene expression levels of CYP4A3, CYP4A8 and CYP1A1 were detected by transcriptome sequencing and qPCR. The internal reference was β-actin.
(B) The gene expression levels of CYP26B1, ALDH1A2 and AOX1 were detected by transcriptome sequencing and qPCR. The internal reference was β-actin. Data are shown as the mean ± SEM of n = 6 per group. Significance: #p < 0.05 vs. control group; ##p < 0.01 vs. control group; ####p < 0.0001 vs. control group; *p < 0.05 vs. ISO group; **p < 0.01 vs. ISO group; ***p < 0.001 vs. ISO group; ****p < 0.0001 vs. ISO group. ISO, isoproterenol-treated group; ISO + AE, ISO + aerobic exercise group; ISO + CA, ISO + canagliflozin; ISO + AE + CA, ISO + aerobic exercise + canagliflozin; ELISA, enzyme linked immunosorbent assay; qPCR, reverse transcription-polymerase chain reaction. Data are represented as mean ± SEM.

pharmacology and whole-transcriptome sequencing, we found that canagliflozin combined with aerobic exercise exerts a protective effect in rats with CHF primarily by modulating the retinol metabolic pathway. The levels of ALDH1A2, CYP26B1, and CYP1A1 on this pathway were significantly up-regulated, while the levels of CYP4A3 and CYP4A8 were down-regulated. In addition, *in vivo* validation experiments have further demonstrated the cardioprotective effect of canagliflozin in combination with aerobic exercise by inhibiting the activation of AKT/ERK pathways.

Accumulating evidence indicates that the pharmacological targeting of the energy metabolic pathways has emerged as a novel therapeutic approach for enhancing cardiac function in a failing heart.[33] Vitamin A (retinol) and its derivatives regulate fundamental biological processes such as development, differentiation, and metabolism,[34] and lipid metabolism were significantly altered in the hearts of retinol-deficient rats. Retinol deprivation is associated with a high level of PPAR expression.[6] PPARs play a crucial role in fatty acid metabolism in the heart and are implicated in the pathogenesis of cardiac hypertrophy and HF. Retinoic acid (RA) is a retinoid derivative that inhibits the progression of myocardial remodeling by modulating the expression of components of the renin-angiotensin system, thereby controlling left ventricular hypertrophy and fibrosis.[35,36] ALDH1A2 is the primary form of RALDHs involved in early embryonic and cardiac development.[37] ALDH1A2 encodes retinal dehydrogenase type 2, which is required for the conversion of dietary retinol to retinoic acid.[38] In cells, retinol is initially reversibly oxidized to retinal,[39] and then retinal is irreversibly converted to retinoic acid. In the GO analysis, responses to retinoic acid and vitamin A were also mentioned. Thus, the retinol metabolic pathway may be critical for the regulation of cardiac energy metabolism in CHF rats when canagliflozin and aerobic exercise are intervened simultaneously.

In this study, the key retinol metabolic pathway indicators CYP4A3, CYP4A8, CYP26B1, and CYP1A1 are members of the cytochrome The cytochrome P450 (P450) family. It is well established that P450 ω-hydroxylases, particularly CYP4A, are involved in Cardiovascular diseases (CVDs).[40] In failing and hypertrophied hearts, CYP4A subfamily expression was found to be upregulated.[41] Previous research has demonstrated that sustained the ISO stimulation of cardiomyocytes increases the expression of CYP4A3, a major CYP450 ω-hydroxylase that generates 20-hydroxyeicosatetraenoic acid (20-HETE) in a time-dependent manner with adverse cardiovascular effects.[40] Inhibition of CYP450 ω-hydroxylase decreased 20-HETE production, protecting cells from ISO-induced apoptosis.[42] Consistent with previous findings, the present study indicates that canagliflozin in combination with aerobic exercise significantly decreased the levels of CYP4A3 and CYP4A8, leading to improvement in heart failure.

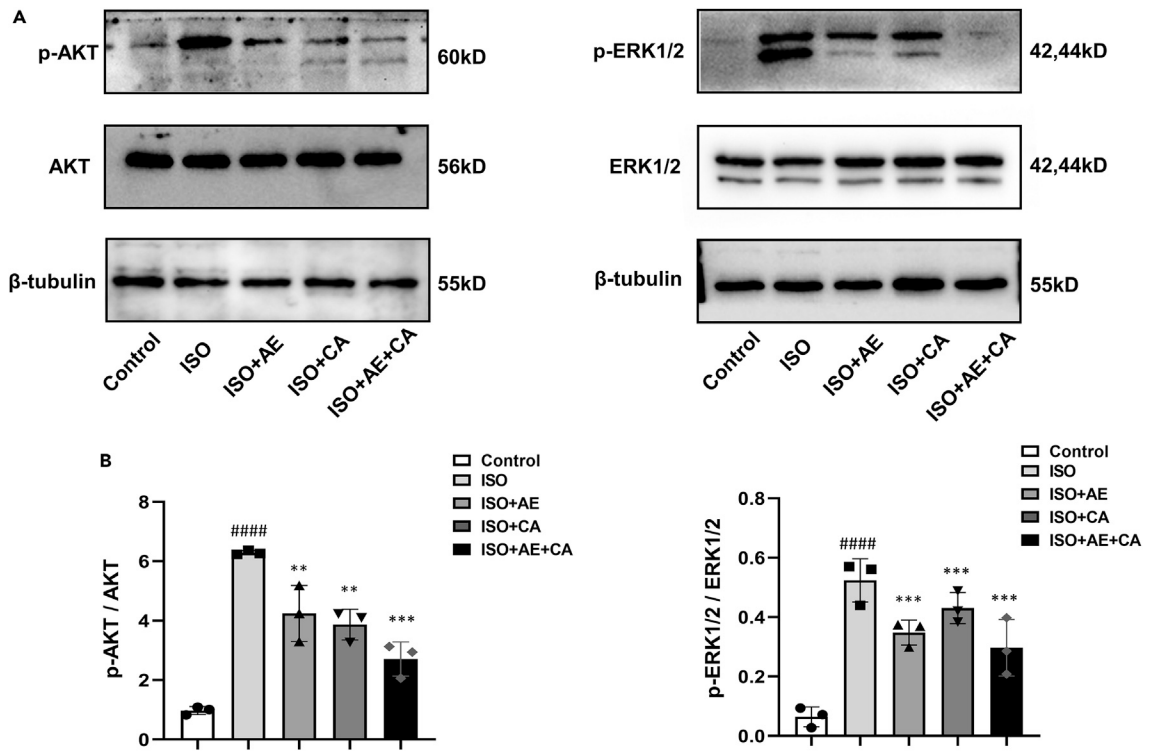

Figure 6. Effects of canagliflozin combined with aerobic exercise on the AKT/ERK signaling pathway in rats

The protein expression levels of AKT, *p*-AKT, ERK1/2 and *p*-ERK1/2 were determined by western blot.

(A) The protein expression levels of AKT, *p*-AKT, ERK1/2 and *p*-ERK1/2 in heart tissues, and β-tubulin was used as the internal standard.

(B) The quantitative results were calculated by Image Lab software. Data are shown as the mean ± SEM of n = 3 per group. Significance: ##p < 0.01 vs. control group; ###p < 0.001 vs. control group; *p < 0.05 vs. ISO group; **p < 0.01 vs. ISO group; ***p < 0.001 vs. ISO group; ****p < 0.0001 vs. ISO group. ISO, isoproterenol-treated group; ISO + AE, ISO + aerobic exercise group; ISO + CA, ISO + canagliflozin; ISO + AE + CA, ISO + aerobic exercise + canagliflozin; *p*-AKT, phosphorylated AKT; *p*-ERK1/2, phosphorylated ERK1/2. Data are represented as mean ± SEM.

The fibrotic response of the heart is a dynamic process in which transforming growth factor β (TGF-β1) is upregulated and activate downstream signals, including AKT and ERK.[29,43] And the PI3K-Akt signaling pathway was downstream of TGF-β1, which significantly stimulated PI3K-Akt signaling pathway activity in cardiac fibroblasts.[43] PI3K is an enzyme that can be activated and catalyze the conversion of phosphatidylinositol diphosphate (PIP2) in the cell membrane to phosphatidylinositol triphosphate (PIP3). AKT is an important cell signaling protein, which is activated by binding to PIP3.[44] Activated AKT further regulates various biological processes, including cell growth, survival, and metabolism. ERK is another important signaling protein. It is a member of the mitogen-activated protein kinase (MAPK) family, involved in the regulation of cell proliferation, differentiation, and survival.[45] TGF-β1 is a cytokine that plays an important role in cell growth, differentiation, migration, and matrix synthesis.[46] TGF-β1 signaling mainly conducts signals by binding to TGF-β receptors on the cell surface and activating Smad proteins. Activated Smad proteins further regulate gene transcription and cellular function. In cell signaling, the PI3K/AKT-ERK signaling pathway and the TGF-β1 signaling pathway can interact. It was shown that PI3K/AKT signaling can promote the production and release of TGF-β1, while also modulate the activation and effects of TGF-β1 signaling.[47] Moreover, TGF-β1 signaling can also affect cell growth and survival by regulating the activation of the PI3K/AKT-ERK signaling pathway.[48] Li et al. discovered that inhibiting AKT/ERK signaling pathways could ameliorate ISO-induced myocardial fibrosis in mice.[29,49,50] Activation of ERK signaling has been shown to induce cardiac hypertrophy, whereas the inhibition of ERK consistently reduces cardiac hypertrophy and fibrosis.[51] Consistent with previous research, we found that the combination of canagliflozin and aerobic exercise significantly decreased the *mRNA* levels of COL1A1, COL3A1, and FN1 and inhibited AKT and ERK phosphorylation. These results suggest that inhibiting the AKT/ERK signaling pathway can ameliorate myocardial fibrosis in rats with ISO.

Conclusions

This study demonstrated that the combination of canagliflozin and aerobic exercise can reduce fibrosis and improve cardiac function by regulating retinol metabolism and the AKT/ERK signaling pathway, thereby exerting a significant protective effect against the development of CHF. Our results provide a rational basis for future clinical studies of canagliflozin in non-diabetic kidney disease. Further understanding of the mechanism of canagliflozin regulation has clinical relevance and provides important insights into the cardio-protective actions of canagliflozin (Figure 7).

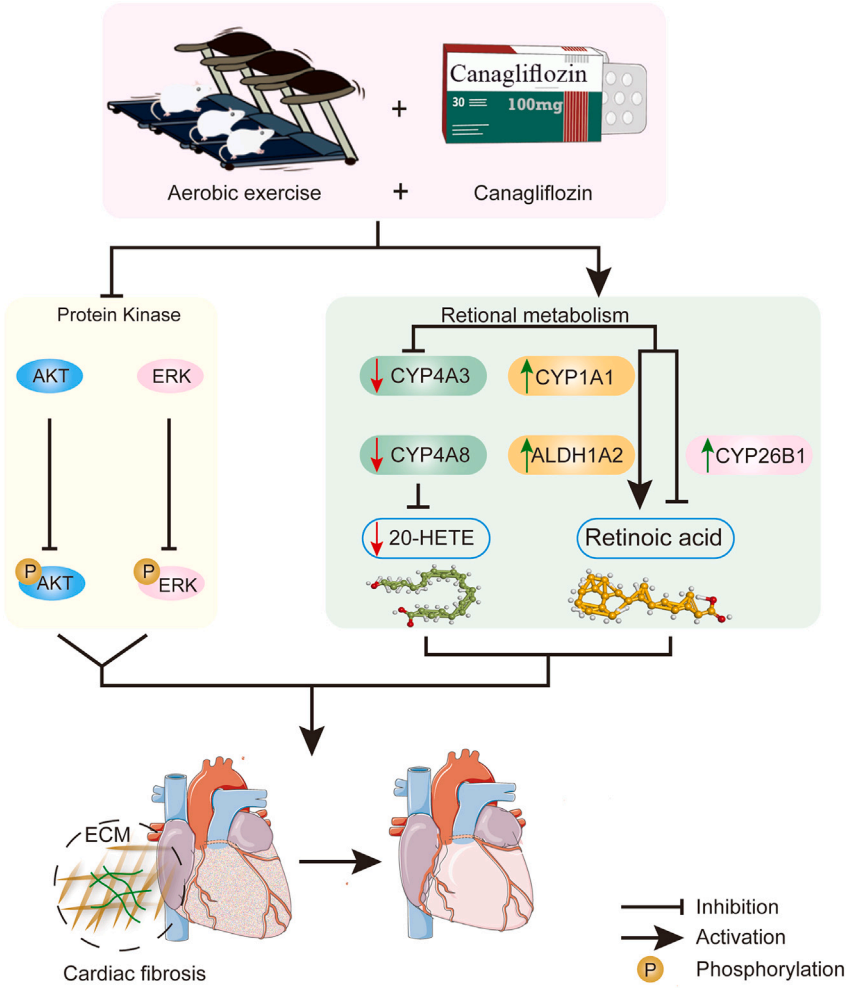

Figure 7. The mechanism of aerobic exercise combined with canagliflozin therapy against ISO-induced CHF

Canagliflozin combined with aerobic exercise therapy modulates protein kinase activity. The combination therapy inhibited the activation of AKT/ERK signaling pathway, thereby improving myocardial fibrosis. Canagliflozin combined with aerobic exercise improved cardiac energy metabolism in CHF rats mainly through the retinol metabolic pathway. The combination significantly upregulated CYP1A1 levels to promote the conversion of retinol to retinoic acid, and it also improved myocardial fibrosis by regulating ALDH1A2 and CYP26B1 to maintain retinoic acid homeostasis. Meanwhile, the combination treatment reduced heart failure by downregulating CYP4A3 and CYP4A8 levels to reduce the production of 20-hydroxyeicosatetraenoic acid.

Clinical perspective

1. Chronic heart failure, the most prevalent form of cardiovascular illness, is a global health issue. Canagliflozin treatment significantly reduced the risk of cardiovascular death, myocardial infarction, and hospitalization for HF in both diabetic and non-diabetic subjects. Heart Failure Guidelines highlight the combination of prescribed medications (SGLT-2 inhibitors) and nonpharmacological therapy for the treatment of CHF. Canagliflozin combined with aerobic exercise may be more beneficial in treating CHF, but the particular effect and molecular mechanism remain unknown.
2. The combination of canagliflozin and aerobic exercise can reduce fibrosis and improve cardiac function by regulating retinol metabolism and the AKT/ERK signaling pathway, thereby exerting a significant protective effect against the development of CHF.
3. Our results provide a rational basis for future clinical studies of canagliflozin in non-diabetic kidney disease. Further understanding of the mechanism of canagliflozin regulation has clinical relevance and provides important insights into the cardio-protective actions of canagliflozin.

Limitations of the study

Although this study provides an in-depth study of the protective role of canagliflozin combined with aerobic exercise in the development of heart failure, there are several limitations. This study used a mouse model, so the findings may not be directly applicable to

humans. Further clinical studies and human trials are still necessary to verify the efficacy and safety of this combination therapy in human patients.

STAR★METHODS

Detailed methods are provided in the online version of this paper and include the following:

- KEY RESOURCES TABLE
- RESOURCE AVAILABILITY
  - Lead contact
  - Material availability
  - Data and code availability

ACKNOWLEDGMENTS

This work was supported by the Natural Science Foundation of China [no. 82000788]; Chinese Postdoc-toral Science Foundation [2021M702040]; Key Research & Development Plan of Shandong Province [no. 2018GSF118176]; Guangdong Basic and Applied Basic Research Foundation [no. 2019A1515110023]; Natural Science Foundation of Shandong Province [no. ZR2016HQ26]; the Bethune-Merck's Diabetes Research Foundation [no. B-0307-H-20200302, G2016014]; Medicine and Health Science and Technology Development Plan of Shandong Province [no. 2018WS201]; and Science and technology plan of Shandong Provincial University [no. J16LK09].

AUTHOR CONTRIBUTIONS

ZZW and YSH contributed to the study conception and preparation of the article. FH, YZD, and WXY contributed to the study conception and design, SHL and DBY drafted the article and gave final approval of the version to be sent.

DECLARATION OF INTERESTS

The authors declare that they have no conflict of interest.

Received: July 5, 2023
Revised: December 1, 2023
Accepted: January 22, 2024
Published: February 15, 2024

REFERENCES

1. Wen, J., Zhang, L., Liu, H., Wang, J., Li, J., Yang, Y., Wang, Y., Cai, H., Li, R., and Zhao, Y. (2019). Salsolinol Attenuates Doxorubicin-Induced Chronic Heart Failure in Rats and Improves Mitochondrial Function in H9c2 Cardiomyocytes. Front. Pharmacol. *10*, 1135. https://doi.org/10.3389/fphar.2019.01135.
2. Zhang, S., Liu, H., Fang, Q., He, H., Lu, X., Wang, Y., and Fan, X. (2021). Shexiang Tongxin Dropping Pill Protects Against Chronic Heart Failure in Mice via Inhibiting the ERK/MAPK and TGF-β Signaling Pathways. Front. Pharmacol. *12*, 796354. https://doi.org/10.3389/fphar.2021.796354.
3. Wang, L., Gao, K., and Wang, D. (2018). Exercise training has restorative potential on myocardial energy metabolism in rats with chronic heart failure. Iran. J. Basic Med. Sci. *21*, 818–823. https://doi.org/10.22038/ijbms.2018.29294.7076.
4. Wu, D., Jian, C., Peng, Q., Hou, T., Wu, K., Shang, B., Zhao, M., Wang, Y., Zheng, W., Ma, Q., et al. (2020). Prohibitin 2 deficiency impairs cardiac fatty acid oxidation and causes heart failure. Cell Death Dis. *11*, 181. https://doi.org/10.1038/s41419-020-2374-7.
5. Bashir, A., Zhang, J., and Denney, T.S. (2020). Creatine kinase rate constant in the human heart at 7T with 1D-ISIS/2D CSI localization. PLoS One *15*, e0229933. https://doi.org/10.1371/journal.pone.0229933.
6. Vega, V.A., Anzulovich, A.C., Varas, S.M., Bonomi, M.R., Giménez, M.S., and Oliveros, L.B. (2009). Effect of nutritional vitamin A deficiency on lipid metabolism in the rat heart: Its relation to PPAR gene expression. Nutrition *25*, 828–838. https://doi.org/10.1016/j.nut.2009.01.008.
7. Saibil, S.D., St Paul, M., Laister, R.C., Garcia-Batres, C.R., Israni-Winger, K., Elford, A.R., Grimshaw, N., Robert-Tissot, C., Roy, D.G., Jones, R.G., et al. (2019). Activation of Peroxisome Proliferator-Activated Receptors α and δ Synergizes with Inflammatory Signals to Enhance Adoptive Cell Therapy. Cancer Res. *79*, 445–451. https://doi.org/10.1158/0008-5472.Can-17-3053.
8. Khuchua, Z., Glukhov, A.I., Strauss, A.W., and Javadov, S. (2018). Elucidating the Beneficial Role of PPAR Agonists in Cardiac Diseases. Int. J. Mol. Sci. *19*, 3464. https://doi.org/10.3390/ijms19113464.
9. Packer, M., Anker, S.D., Butler, J., Filippatos, G., Ferreira, J.P., Pocock, S.J., Carson, P., Anand, I., Doehner, W., Haass, M., et al. (2021). Effect of Empagliflozin on the Clinical Stability of Patients With Heart Failure and a Reduced Ejection Fraction: The EMPEROR-Reduced Trial. Circulation *143*, 326–336. https://doi.org/10.1161/circulationaha.120.051783.
10. McDonald, M., Virani, S., Chan, M., Ducharme, A., Ezekowitz, J.A., Giannetti, N., Heckman, G.A., Howlett, J.G., Koshman, S.L., Lepage, S., et al. (2021). CCS/CHFS Heart Failure Guidelines Update: Defining a New Pharmacologic Standard of Care for Heart Failure With Reduced Ejection Fraction. Can. J. Cardiol. *37*, 531–546. https://doi.org/10.1016/j.cjca.2021.01.017.
11. Aragón-Herrera, A., Feijóo-Bandín, S., Otero Santiago, M., Barral, L., Campos-Toimil, M., Gil-Longo, J., Costa Pereira, T.M., García-Caballero, T., Rodríguez-Segade, S., Rodríguez, J., et al. (2019). Empagliflozin reduces the levels of CD36 and cardiotoxic lipids while improving autophagy in the hearts of Zucker diabetic fatty rats. Biochem. Pharmacol. *170*, 113677. https://doi.org/10.1016/j.bcp.2019.113677.
12. Takada, S., Sabe, H., and Kinugawa, S. (2022). Treatments for skeletal muscle abnormalities in heart failure: sodium-glucose transporter 2 and ketone bodies. Am. J. Physiol. Heart Circ. Physiol. *322*, H117–H128. https://doi.org/10.1152/ajpheart.00100.2021.
13. Baker, H.E., Kiel, A.M., Luebbe, S.T., Simon, B.R., Earl, C.C., Regmi, A., Roell, W.C., Mather, K.J., Tune, J.D., and Goodwill, A.G. (2019). Inhibition of sodium-glucose cotransporter-2 preserves cardiac function during regional myocardial ischemia independent of alterations in myocardial substrate utilization. Basic Res. Cardiol. *114*,

25. https://doi.org/10.1007/s00395-019-0733-2.
14. He, L., Ma, S., Zuo, Q., Zhang, G., Wang, Z., Zhang, T., Zhai, J., and Guo, Y. (2022). An Effective Sodium-Dependent Glucose Transporter 2 Inhibition, Canagliflozin, Prevents Development of Hypertensive Heart Failure in Dahl Salt-Sensitive Rats. Front. Pharmacol. *13*, 856386. https://doi.org/10.3389/fphar.2022.856386.
15. Konopka, A.R., and Harber, M.P. (2014). Skeletal muscle hypertrophy after aerobic exercise training. Exerc. Sport Sci. Rev. *42*, 53–61. https://doi.org/10.1249/jes.0000000000000007.
16. Gomes, M.J., Pagan, L.U., Lima, A.R.R., Reyes, D.R.A., Martinez, P.F., Damatto, F.C., Pontes, T.H.D., Rodrigues, E.A., Souza, L.M., Tosta, I.F., et al. (2020). Effects of aerobic and resistance exercise on cardiac remodelling and skeletal muscle oxidative stress of infarcted rats. J. Cell Mol. Med. *24*, 5352–5362. https://doi.org/10.1111/jcmm.15191.
17. Bozkurt, B., Fonarow, G.C., Goldberg, L.R., Guglin, M., Josephson, R.A., Forman, D.E., Lin, G., Lindenfeld, J., O'Connor, C., Panjrath, G., et al. (2021). Cardiac Rehabilitation for Patients With Heart Failure: JACC Expert Panel. J. Am. Coll. Cardiol. *77*, 1454–1469. https://doi.org/10.1016/j.jacc.2021.01.030.
18. Stølen, T., Shi, M., Wohlwend, M., Høydal, M.A., Bathen, T.F., Ellingsen, Ø., and Esmaeili, M. (2020). Effect of exercise training on cardiac metabolism in rats with heart failure. Scand. Cardiovasc. J. *54*, 84–91. https://doi.org/10.1080/14017431.2019.1658893.
19. Xie, C., Zhang, Y., Tran, T.D.N., Wang, H., Li, S., George, E.V., Zhuang, H., Zhang, P., Kandel, A., Lai, Y., et al. (2015). Irisin Controls Growth, Intracellular Ca2+ Signals, and Mitochondrial Thermogenesis in Cardiomyoblasts. PLoS One *10*, e0136816. https://doi.org/10.1371/journal.pone.0136816.
20. Keihanian, F., Moohebati, M., Saeidinia, A., Mohajeri, S.A., and Madaeni, S. (2021). Therapeutic effects of medicinal plants on isoproterenol-induced heart failure in rats. Biomed. Pharmacother. *134*, 111101. https://doi.org/10.1016/j.biopha.2020.111101.
21. Liu, M., Ai, J., Feng, J., Zheng, J., Tang, K., Shuai, Z., and Yang, J. (2019). Effect of paeoniflorin on cardiac remodeling in chronic heart failure rats through the transforming growth factor β1/Smad signaling pathway. Cardiovasc. Diagn. Ther. *9*, 272–280. https://doi.org/10.21037/cdt.2019.06.01.
22. Hira, T., Koga, T., Sasaki, K., and Hara, H. (2017). Canagliflozin potentiates GLP-1 secretion and lowers the peak of GIP secretion in rats fed a high-fat high-sucrose diet. Biochem. Biophys. Res. Commun. *492*, 161–165. https://doi.org/10.1016/j.bbrc.2017.08.031.
23. Bedford, T.G., Tipton, C.M., Wilson, N.C., Oppliger, R.A., and Gisolfi, C.V. (1979). Maximum oxygen consumption of rats and its changes with various experimental procedures. J. Appl. Physiol. Respir. Environ. Exerc. Physiol. *47*, 1278–1283. https://doi.org/10.1152/jappl.1979.47.6.1278.
24. Szklarczyk, D., Gable, A.L., Nastou, K.C., Lyon, D., Kirsch, R., Pyysalo, S., Doncheva, N.T., Legeay, M., Fang, T., Bork, P., et al. (2021). The STRING database in 2021: customizable protein-protein networks, and functional characterization of user-uploaded gene/measurement sets. Nucleic Acids Res. *49*, D605–D612. https://doi.org/10.1093/nar/gkaa1074.
25. Bader, G.D., and Hogue, C.W.V. (2003). An automated method for finding molecular complexes in large protein interaction networks. BMC Bioinf. *4*, 2. https://doi.org/10.1186/1471-2105-4-2.
26. Shannon, P., Markiel, A., Ozier, O., Baliga, N.S., Wang, J.T., Ramage, D., Amin, N., Schwikowski, B., and Ideker, T. (2003). Cytoscape: a software environment for integrated models of biomolecular interaction networks. Genome Res. *13*, 2498–2504. https://doi.org/10.1101/gr.1239303.
27. Zhou, Y., Zhou, B., Pache, L., Chang, M., Khodabakhshi, A.H., Tanaseichuk, O., Benner, C., and Chanda, S.K. (2019). Metascape provides a biologist-oriented resource for the analysis of systems-level datasets. Nat. Commun. *10*, 1523. https://doi.org/10.1038/s41467-019-09234-6.
28. Wang, L., Tian, X., Cao, Y., Ma, X., Shang, L., Li, H., Zhang, X., Deng, F., Li, S., Guo, T., and Yang, P. (2021). Cardiac Shock Wave Therapy Improves Ventricular Function by Relieving Fibrosis Through PI3K/Akt Signaling Pathway: Evidence From a Rat Model of Post-infarction Heart Failure. Front. Cardiovasc. Med. *8*, 693875. https://doi.org/10.3389/fcvm.2021.693875.
29. Li, L., Fang, H., Yu, Y.H., Liu, S.X., and Yang, Z.Q. (2021). Liquiritigenin attenuates isoprenaline-induced myocardial fibrosis in mice through the TGF-β1/Smad2 and AKT/ERK signaling pathways. Mol. Med. Rep. *24*, 686. https://doi.org/10.3892/mmr.2021.12326.
30. Gallo, S., Vitacolonna, A., Bonzano, A., Comoglio, P., and Crepaldi, T. (2019). ERK: A Key Player in the Pathophysiology of Cardiac Hypertrophy. Int. J. Mol. Sci. *20*, 2164. https://doi.org/10.3390/ijms20092164.
31. Sussman, M.A., Völkers, M., Fischer, K., Bailey, B., Cottage, C.T., Din, S., Gude, N., Avitabile, D., Alvarez, R., Sundararaman, B., et al. (2011). Myocardial AKT: the omnipresent nexus. Physiol. Rev. *91*, 1023–1070. https://doi.org/10.1152/physrev.00024.2010.
32. Lu, M., Qin, Q., Yao, J., Sun, L., and Qin, X. (2019). Induction of LOX by TGF-β1/Smad/AP-1 signaling aggravates rat myocardial fibrosis and heart failure. IUBMB Life *71*, 1729–1739. https://doi.org/10.1002/iub.2112.
33. Lopaschuk, G.D., Karwi, Q.G., Tian, R., Wende, A.R., and Abel, E.D. (2021). Cardiac Energy Metabolism in Heart Failure. Circ. Res. *128*, 1487–1513. https://doi.org/10.1161/circresaha.121.318241.
34. Chen, C.H., Ke, L.Y., Chan, H.C., Lee, A.S., Lin, K.D., Chu, C.S., Lee, M.Y., Hsiao, P.J., Hsu, C., Chen, C.H., and Shin, S.J. (2016). Electronegative low density lipoprotein induces renal apoptosis and fibrosis: STRA6 signaling involved. J. Lipid Res. *57*, 1435–1446. https://doi.org/10.1194/jlr.M067215.
35. Ono, K., Sandell, L.L., Trainor, P.A., and Wu, D.K. (2020). Retinoic acid synthesis and autoregulation mediate zonal patterning of vestibular organs and inner ear morphogenesis. Development *147*. https://doi.org/10.1242/dev.192070.
36. Choudhary, R., Palm-Leis, A., Scott, R.C., 3rd, Guleria, R.S., Rachut, E., Baker, K.M., and Pan, J. (2008). All-trans retinoic acid prevents development of cardiac remodeling in aortic banded rats by inhibiting the renin-angiotensin system. Am. J. Physiol. Heart Circ. Physiol. *294*, H633–H644. https://doi.org/10.1152/ajpheart.01301.
37. Pavan, M., Ruiz, V.F., Silva, F.A., Sobreira, T.J., Cravo, R.M., Vasconcelos, M., Marques, L.P., Mesquita, S.M.F., Krieger, J.E., Lopes, A.A.B., et al. (2009). ALDH1A2 (RALDH2) genetic variation in human congenital heart disease. BMC Med. Genet. *10*, 113. https://doi.org/10.1186/1471-2350-10-113.
38. Steiner, M.B., Vengoechea, J., and Collins, R.T., 2nd (2013). Duplication of the ALDH1A2 gene in association with pentalogy of Cantrell: a case report. J. Med. Case Rep. *7*, 287. https://doi.org/10.1186/1752-1947-7-287.
39. Sandell, L.L., Sanderson, B.W., Moiseyev, G., Johnson, T., Mushegian, A., Young, K., Rey, J.P., Ma, J.X., Staehling-Hampton, K., and Trainor, P.A. (2007). RDH10 is essential for synthesis of embryonic retinoic acid and is required for limb, craniofacial, and organ development. Genes Dev. *21*, 1113–1124. https://doi.org/10.1101/gad.1533407.
40. Roman, R.J. (2002). P-450 metabolites of arachidonic acid in the control of cardiovascular function. Physiol. Rev. *82*, 131–185. https://doi.org/10.1152/physrev.00021.2001.
41. Althurwi, H.N., Elshenawy, O.H., and El-Kadi, A.O.S. (2014). Fenofibrate modulates cytochrome P450 and arachidonic acid metabolism in the heart and protects against isoproterenol-induced cardiac hypertrophy. J. Cardiovasc. Pharmacol. *63*, 167–177. https://doi.org/10.1097/fjc.0000000000000036.
42. Jiang, S., Huo, D., Wang, X., Zhao, H., Tan, J., Zeng, Q., O'Rourke, S.T., and Sun, C. (2017). β-adrenergic Receptor-stimulated Cardiac Myocyte Apoptosis: Role of Cytochrome P450 ω-hydroxylase. J. Cardiovasc. Pharmacol. *70*, 94–101. https://doi.org/10.1097/fjc.0000000000000499.
43. Zeng, Z., Wang, Q., Yang, X., Ren, Y., Jiao, S., Zhu, Q., Guo, D., Xia, K., Wang, Y., Li, C., and Wang, W. (2019). Qishen granule attenuates cardiac fibrosis by regulating TGF-β/Smad3 and GSK-3β pathway. Phytomedicine *62*, 152949. https://doi.org/10.1016/j.phymed.2019.152949.
44. Badolia, R., Manne, B.K., Dangelmaier, C., Chernoff, J., and Kunapuli, S.P. (2015). Gq-mediated Akt translocation to the membrane: a novel PIP3-independent mechanism in platelets. Blood *125*, 175–184. https://doi.org/10.1182/blood-2014-05-576306.
45. Ruppert, C., Deiss, K., Herrmann, S., Vidal, M., Oezkur, M., Gorski, A., Weidemann, F., Lohse, M.J., and Lorenz, K. (2013). Interference with ERK(Thr188) phosphorylation impairs pathological but not physiological cardiac hypertrophy. Proc. Natl. Acad. Sci. USA *110*, 7440–7445. https://doi.org/10.1073/pnas.1221999110.
46. Redondo, S., Santos-Gallego, C.G., and Tejerina, T. (2007). TGF-beta1: a novel target for cardiovascular pharmacology. Cytokine Growth Factor Rev. *18*, 279–286. https://doi.org/10.1016/j.cytogfr.2007.04.005.
47. Lee, K.S., Park, S.J., Kim, S.R., Min, K.H., Lee, K.Y., Choe, Y.H., Hong, S.H., Lee, Y.R., Kim, J.S., Hong, S.J., and Lee, Y.C. (2008). Inhibition of VEGF blocks TGF-beta1 production through a PI3K/Akt signalling

pathway. Eur. Respir. J. *31*, 523–531. https://doi.org/10.1183/09031936.00125007.

48. Tang, Q., Markby, G.R., MacNair, A.J., Tang, K., Tkacz, M., Parys, M., Phadwal, K., MacRae, V.E., and Corcoran, B.M. (2023). TGF-β-induced PI3K/AKT/mTOR pathway controls myofibroblast differentiation and secretory phenotype of valvular interstitial cells through the modulation of cellular senescence in a naturally occurring in vitro canine model of myxomatous mitral valve disease. Cell Prolif. *56*, e13435. https://doi.org/10.1111/cpr.13435.
49. Wei, W.Y., Ma, Z.G., Xu, S.C., Zhang, N., and Tang, Q.Z. (2016). Pioglitazone Protected against Cardiac Hypertrophy via Inhibiting AKT/GSK3β and MAPK Signaling Pathways. PPAR Res. *2016*, 9174190. https://doi.org/10.1155/2016/9174190.
50. Gao, G., Jiang, S., Ge, L., Zhang, S., Zhai, C., Chen, W., and Sui, S. (2019). Atorvastatin Improves Doxorubicin-Induced Cardiac Dysfunction by Modulating Hsp70, Akt, and MAPK Signaling Pathways. J. Cardiovasc. Pharmacol. *73*, 223–231. https://doi.org/10.1097/fjc.0000000000000646.
51. Tao, H., Xu, W., Qu, W., Gao, H., Zhang, J., Cheng, X., Liu, N., Chen, J., Xu, G.L., Li, X., and Shu, Q. (2021). Loss of ten-eleven translocation 2 induces cardiac hypertrophy and fibrosis through modulating ERK signaling pathway. Hum. Mol. Genet. *30*, 865–879. https://doi.org/10.1093/hmg/ddab046.

STAR★METHODS

KEY RESOURCES TABLE

REAGENT or RESOURCE	SOURCE	IDENTIFIER
Antibodies		
β-tubulin	Proteintech	10068-1-AP
AKT	Abcam	cat. no. ab32505
phosphorylated AKT	Abcam	cat. no. ab192623
ERK1/2	Abcam	cat. no. ab184699
phosphorylated ERK1/2	Abcam	cat. no. ab201015;
Biological samples		
heart tissue (rat)	This paper	N/A
Experimental models: Organisms/strains		
Mouse: Male Sprague Dawley (SD)	Beijing Weitong 99 Lihua Laboratory Animal Technology Co., Ltd.	002
Oligonucleotides		
R-COL1A1-S		CCCAGCGGTGGTTATGACTT
R-COL1A1-A		TCGATCCAGTACTCTCCGCT
R-COL3A1-S		CGAGGTAACAGAGGTGAAAGAGG
R-COL3A1-A		TTTCACCTCCAACTCCAGCAAT
R-FN1-S		AAACCTCTACGGGTCGCTG
R-FNI-A		GCGCTGGTGGTGAAGTCAAA
R-CYP1A1-S		GACATTTGAGAAGGGCCACATC
R-CYP1A1-A		GGTTGGTTACCAGGTACATGAGG
R-CYP2C23-S		AGAACTTGGCTGTCTGTGGGTC
R-CYP2C23-A		TCGGTATAAGGCAGCTTCATCT
R-ALDH1A2-S		TGGACGCTTCTGAAAGAGGAC
R-ALDH1A2-A		GGCTTACCGCCATTTAGTGATT
R-CYP4A8-S		CAGCACCGACGAATGTTGACT
R-CYP4A8-A		AACTGGACACTGCCCTCTTGG
R-CYP4A3-S		TGCTCAGTCTATTTCTGGTGCTG
R-CYP4A3-A		CCACGTAAGAACCTGCTGGAAT
R-CYP26B1-S		AGAGCTGCAAGCTGCCTATCC
R-CYP26B1-A		CTGGTGTTCGCCCAGTAGGAT
RB-ACTINS		TGCTATGTTGCCCTAGACTTCG
RB-ACTIN-A		GTTGGCATAGAGGTCTTTACGG
Software and algorithms		
ImageJ	National Institutes of Health	https://imagej.nih.gov/ij/
Cytoscape	Bloomage Biotechnol Corporation	3.7.1
GraphPad Prism 8	GraphPad	N/A

RESOURCE AVAILABILITY

Lead contact

Further information and requests for resources and reagents should be directed to and will be fulfilled by the lead contact, Zhongwen Zhang (zhangzhongwen@sdu.edu.cn).

Material availability

This study did not generate any new unique reagents.

Data and code availability

All relevant data for this study are available from the corresponding authors (accession number GSE225149). This paper does not report original code. Any additional information required to reanalyze the data reported in this paper is available from the lead contact upon request. The data used to support the findings of this study are available from the corresponding author upon request.